# Spin-polarized current and tunneling magnetoresistance in ferromagnetic gate bilayer graphene structures

V. Hung Nguyen,[1,2,a)] A. Bournel,[1] and P. Dollfus[1]
[1]*Institut d'Electronique Fondamentale, UMR8622, CNRS, Université Paris Sud, 91405 Orsay, France*
[2]*Center for Computational Physics, Institute of Physics, VAST, P.O. Box 429 Bo Ho, Hanoi 10000, Vietnam*

(Received 15 December 2010; accepted 18 February 2011; published online 7 April 2011)

We study spin transport in bilayer graphene structures where gate electrodes are attached to ferromagnetic graphene. Due to the exchange field in the gated regions, the current becomes spin dependent and can be controlled by tuning the gate voltages. It is shown that thanks to strong resonant chiral tunneling inherent in bilayer graphene, very high spin polarization and tunneling magnetoresistance can be achieved in the considered structures. Different possibilities for controlling the spin current are discussed. The study demonstrates the potential of bilayer graphene structures for spintronic applications with significant improvement over previously predicted results in monolayer graphene structures. © *2011 American Institute of Physics*. [doi:10.1063/1.3569621]

## I. INTRODUCTION

Since its first isolation in 2004,[1] graphene has drawn rapidly growing interest for its fascinating characteristics and various potential applications.[2–5] This results in particular from its specific gapless electronic structure[6] and some attractive properties such as high carrier mobility[7] and small spin-orbit coupling.[8] A number of unusual transport phenomena, such as finite minimal conductivity,[9] an unconventional quantum Hall effect,[10] the Klein paradox,[11] etc., have been demonstrated and explored. The potential of graphene for high performance electronic devices has been discussed (e.g., see a recent review[4]). Moreover, graphene also appears to be very promising for spintronic applications, as discussed, for instance, in Ref. 5. This is because its long spin relaxation length[12] makes graphene an excellent candidate for use in ballistic spin transport, and the possibilities of inducing magnetism in graphene[13–17] provide a multiform controllability of spin current in graphene-based structures. On the basis of such considerations, several approaches for controlling the spin transport in graphene nanostructures have been proposed. For instance, the spin polarized states induced by a transverse electric field and/or the edge defect in zigzag graphene nanoribbons have been discussed in a number of works.[15,18–20] In addition, the possibility of controlling the spin polarized current using a ferromagnetic gate has been predicted and is discussed in detail in Refs. 21–25. It was shown that due to the spin splitting induced in ferromagnetic graphene and to the chiral tunneling through hole bound states in the barrier region, a spin polarized current is generated and has an oscillatory behavior with respect to the barrier height, which can be tuned by the gate voltage. Though the features observed are very interesting, these structures have some drawbacks in terms of practical use. In particular, due to their zero energy bandgap, the spin polarization in 2D-monolayer graphene structures is limited,[21–23] i.e., it is always smaller than 30%. As a possible way of overcoming this limitation, the spin polarization effect can be improved in armchair graphene nanoribbon structures with a finite energy bandgap and/or with the use of normal conducting leads.[24,25] However, it has been shown that the results obtained are very sensitive to the device geometry, e.g., the device length and the edge effects.

In recent works,[26,27] we have found that due to their specific electronic structure, the device operation of bilayer graphene structures is better than that of monolayer structures. In particular, strong resonant tunneling effects and significant negative differential conductance behavior have been demonstrated (Ref. 26). In addition, it was shown that the electric-field-induced energy bandgap provides a possible way to switch off the electrical current,[27] which is necessary for digital applications (see more in Refs. 28 and 29). On this basis, it is expected that the spin polarization effect in ferromagnetic structures based on bilayer graphene can be improved in comparison with that in monolayer structures. In this work, using the nonequilibrium Green's function method (NEGF),[26,27] we investigate the spin transport in bilayer graphene structures wherein, as illustrated in Fig. 1, ferromagnetic gates are used to generate and electrostatically control the spin current. We focus on the possibilities of controlling both the spin polarization and the tunneling magnetoresistance using different gate configurations, as shown in Fig. 1.

## II. MODEL AND CALCULATION

To describe the charge states in bilayer graphene, a simple nearest neighbor tight binding model conveniently can be used,[3] with $a_c = 0.142$ nm as the carbon–carbon distance and $t = 2.7$ eV and $\gamma = 0.39$ eV as the hopping energies inside and between the graphene layers, respectively. By expanding the momentum close to the K-points in the Brillouin zone, the energy dispersion can be written as

$$E^2 = \hbar^2 v_F^2 k^2 + \frac{\gamma^2}{2} + \frac{\Delta^2}{4} \pm \sqrt{\left(\gamma^2 + \Delta^2\right)\hbar^2 v_F^2 k^2 + \frac{\gamma^4}{4}}, \quad (1)$$

[a)]Author to whom correspondence should be addressed. Electronic mail: viet-hung.nguyen@u-psud.fr.

 © 2011 American Institute of Physics

Author complimentary copy. Redistribution subject to AIP license or copyright, see http://jap.aip.org/jap/copyright.jsp

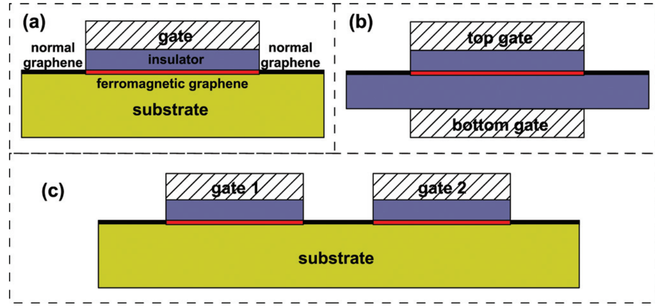


FIG. 1. (Color online) Model of considered ferromagnetic gate graphene structures wherein the ferromagnetic graphene can be generated intrinsically by doping and defects (Refs. 13 and 14), or extrinsically by the exchange interaction with the ferromagnetic insulator (Refs. 16 and 17). The gate electrodes are used to modulate electrostatically the magnitude of the spin current.

where $v_F = 3a_c t/2\hbar \approx 10^6$ m/s is the Fermi velocity of the monolayer modes, and $\Delta = U_1 - U_2$ stands for the potential difference between the graphene layers. When $\Delta = 0$ and $\hbar v_F k \ll \gamma$, the energy dispersion may be simplified as $E(\vec{k}) = \pm\hbar^2 k^2/2m$ with the effective mass $m = \gamma/2v_F^2$. This is definitely different from the case of monolayer graphene, wherein the energy dispersion is linear around the K-points. The Hamiltonian of such a structure simply reads

$$H = \begin{bmatrix} v_F\vec{\sigma}\vec{p} & \tau \\ \tau^\dagger & v_F\vec{\sigma}\vec{p} + U_2 \end{bmatrix}, \quad \tau = \begin{bmatrix} 0 & 0 \\ \gamma & 0 \end{bmatrix}. \tag{2}$$

We assume that the potential energies are just functions of $x$ (OX is the transport direction). To solve this problem, an efficient calculation method based on the NEGF formalism has been developed by rewriting the Hamiltonian equation (2) within a tight binding formulation in a new basis $\{|x_n\rangle, |k_y\rangle\}$ using the arbitrary mesh spacing $x_{n+1} - x_n = a_0$.[26,27] Throughout the work, $a_0$ has a chosen value of 0.2 nm, which is proved to be small enough to give accurate results. The device retarded Green's function is then defined as

$$G^r(E) = [E + i\eta - H - \Sigma_L - \Sigma_R]^{-1}, \tag{3}$$

where $\Sigma_{L(R)}$ is the left (right) contact-to-device coupling self-energy, which can be solved using the fast iterative scheme[30] as presented in Ref. 27. The transmission coefficient and the conductance are given by

$$\mathcal{T} = \mathrm{Tr}\left[\Gamma_L G^r \Gamma_R G^{r\dagger}\right], \tag{4}$$

$$G = \frac{2e^2 W}{\pi h}\int_{-\infty}^{\infty} dE dk_y \mathcal{T}(E, k_y)\left(-\frac{\partial f}{\partial E}\right), \tag{5}$$

in which $\Gamma_{L(R)} = i(\Sigma_{L(R)} - \Sigma^\dagger_{L(R)})$ is the tunneling rate for the left (right) contact, $W$ is the width of the graphene sheet, $f(E) = \{1 + \exp[(E - E_F)/k_B T]\}^{-1}$ is the Fermi distribution function, and $E_F$ is the Fermi energy. Throughout the work, unless otherwise stated, our simulation is performed at zero temperature.

Note that due to the exchange field of the ferromagnetic graphene, the potential energy in the gated regions, which is normally tuned by the gate voltage, becomes spin dependent. As introduced above, such an exchange field can be induced in graphene intrinsically by doping and defects,[13,14] or extrinsically by the exchange interaction with a ferromagnetic insulator.[16,17] In principle, this may result in a substantial amount of disorder and a nonhomogeneous magnetic field near the gate edges. However, on one hand, the disorder very strongly affects the electronic characteristics when the graphene sheets are narrow;[2,31] therefore, we assume that disorder effects can be negligible in this work where we consider the transport in wide systems.[32] On the other hand, the effects of a magnetic field are important when its magnitude is high and the length of the region in which it appears is large enough.[33] With the assumption that the nonhomogeneous magnetic field is small and appears only in a narrow region, the effect of such a magnetic field is also neglected in our simulation. The potential energy of the device is modeled simply as $U_\sigma(x) = (U_g - \sigma h)\,\theta(x)\,\theta(L - x)$ for the structure in Fig. 1(a) and

$$U_\sigma(x) = \left(U_{g1} - \sigma h_1\right)\theta(x)\,\theta(L_1 - x) + \left(U_{g2} - \sigma h_2\right)\theta(x - L_1 - d)\,\theta(L_1 + L_2 + d - x)$$

in Fig. 1(c), where $U_{g\alpha}$, $h_\alpha$, $L_\alpha$ ($\alpha = 1, 2$), and $d$ are the potential barrier, the exchange splitting energy, the gate length, and the distance between two gate electrodes, respectively. Our study addresses the ballistic spin transport without the spin-flip processes; then the conductance for two spin channels can be considered independently. The spin polarization $P = (G_\uparrow - G_\downarrow)/(G_\uparrow + G_\downarrow)$ and the tunneling magnetoresistance $\mathrm{TMR} = (G_\mathrm{P} - G_\mathrm{AP})/(G_\mathrm{P} + G_\mathrm{AP})$, where $G_{\uparrow(\downarrow)}$ denotes the conductance for the up (down) spin channel and $G_{\mathrm{P(AP)}}$ is the total conductance of the parallel (antiparallel) alignment configuration of magnetic moments.

## III. RESULTS AND DISCUSSION

Using the formalism described above, we now investigate the spin polarized current in single ferromagnetic gate structures [see Fig. 1(a)]. At first, to illustrate the chiral tunneling in bilayer graphene structures, we display the transmission coefficient and a map of the local density of states in Figs. 2(a) and 2(b), respectively. These results are plotted for a finite transverse energy $E_y = 50$ meV ($E_y \equiv \hbar v_F k_y$) and a nonferromagnetic gate ($h = 0$). Figure 2(a) shows many high peaks of $\mathcal{T}$ with very clear gaps in the energy region $E < U_g$. This can be explained as a consequence of the good matching of electron states and hole bound states outside/inside the barrier region (transmission peaks) and the appearance of evanescent states (clear energy gaps) as illustrated in Fig. 2(b). This feature essentially results in strong resonant effects (discussed in detail in Ref. 26), which are also derived from the Fabry–Pérot resonance[34] and manifest clearly through the oscillations of conductance with respect to the barrier height shown in Fig. 2(c). Now, when an exchange field is induced in the gated region, the potential barrier becomes spin dependent and the conductance of each spin channel is shifted relatively to the other, as is illustrated in Fig. 2(c) and similarly discussed in monolayer structures.[17,21,22,24] This essentially leads to the oscillation of the spin polarization when tuning the barrier height [see Fig. 2(d)]. The strong

Author complimentary copy. Redistribution subject to AIP license or copyright, see http://jap.aip.org/jap/copyright.jsp

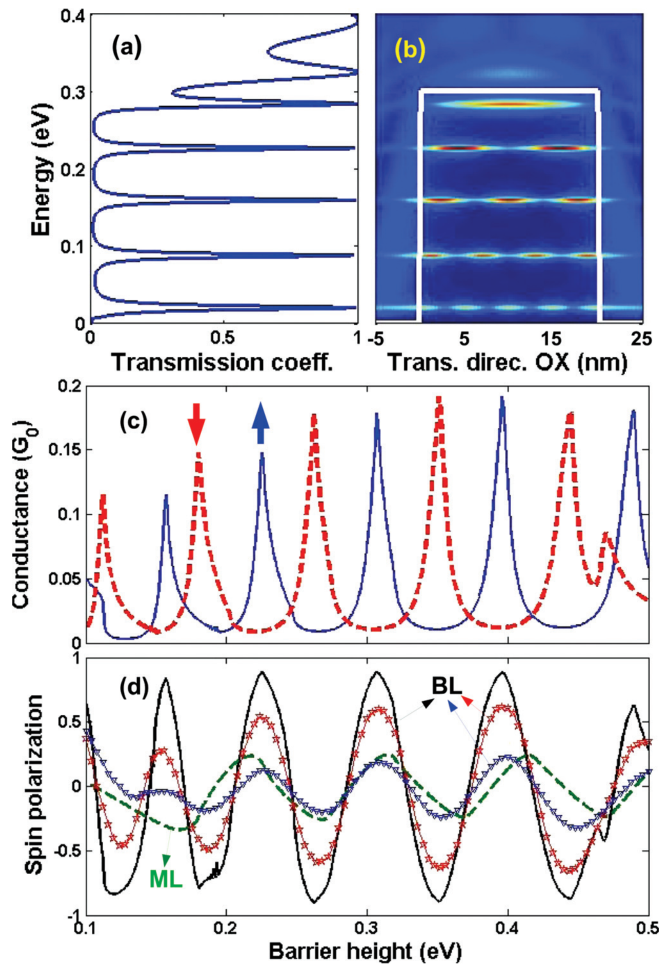


FIG. 2. (Color online) (a) Transmission coefficient and (b) local density of states plotted for $E_y = 50$ meV clearly showing the picture of chiral tunneling in single barrier bilayer graphene structures for $h = 0$ (Ref. 26). Oscillation of (c) the conductance $G_\sigma$ ($\sigma = \uparrow, \downarrow$) and (d) the spin polarization $P$ (solid curve) vs the barrier height $U_g$ in the single ferromagnetic gate structure. In (d), the solid, (star, solid), and ($\nabla$, solid) curves are obtained at $T = 0$, 77, and 150 K, respectively, and the dashed line corresponds to the results obtained in the monolayer structure (Ref. 22) with the same parameters at $T = 0$ K. The Fermi energy $E_F = 75$ meV, the spin splitting $h = 22.5$ meV, and the gate length $L = 20$ nm. The conductance is given in the unit of $G_0 = e^2 W / 2\pi h a_0$.

resonant effects seen in Figs. 2(a)–2(c) therefore result in a very high spin polarization in this structure—it reaches 90% [solid curve in Fig. 2(d)] at zero temperature, while its maximum value is only about 30% in monolayer structures [see Refs. 21–23 or the dashed curve in Fig. 2(d)]. It is worth noting that even at finite temperature, the spin polarization in bilayer graphene structures is still significant; magnitudes as high as about 60% and 30% are achieved at 77K and 150K [(star, solid) and ($\nabla$, solid) curves in Fig. 2(d)], respectively. Moreover, our study also shows that the period of such oscillations is proportional to $1/L$. This implies an unusual quantization of charge states in graphene-based structures.[22,24,26]

Other means of controlling the spin polarized current can be achieved by taking advantage of the electric-field-induced energy bandgap, e.g., as mentioned in Refs. 29 and 35. Due to such a feature, various band alignments, which lead to different types of heterostructures, can be realized in bilayer graphene.[36] Here, we propose to use a simple structure (double gate structure) as shown in Fig. 1(b) to efficiently control the spin current. As is discussed in Ref. 27, a finite energy bandgap in the gated region results in a conduction gap around its potential energy. Therefore, one can expect that when inducing a spin splitting in the structure, the current for one spin channel is switched off and a perfect spin polarization can be achieved. Indeed, this idea is confirmed and illustrated very clearly in Fig. 3, where we plot the spin polarization as a function of the potential energy $U_g$ around the Fermi level for different values of $\Delta$. Note that in this situation, $U_{1\sigma} = U_g + \Delta/2 - \sigma h$ and $U_{2\sigma} = U_g - \Delta/2 - \sigma h$ are assumed to be the potential energy (for the spin channel $\sigma$) in layers 1 and 2, respectively. It is shown that a peak in the region $U_g < E_F$ and a valley in the region $U_g > E_F$, where the spin polarization can tend toward 100%, are observed, and the energy spacing between them increases with an increase in the potential difference $\Delta$. This result suggests an efficient way of switching the spin polarization with perfect values by tuning the potential energy $U_g$ around the Fermi level.

Now, we consider the spin transport in dual gate structures with two gates in series [see Fig. 1(c)]. As is discussed in Ref. 37, the charge transport in the double barrier monolayer structures depends very strongly on the hole bound states in both barriers. Therefore, the oscillation of the conductance with respect to the height of one barrier is modulated periodically when changing the height of the other one. Based on this, we first present in Fig. 4 the total conductance and the spin polarization as a function of the barrier height $U_{g1}$ (ferromagnetic gate) for different values of $U_{g2}$ (normal gate). It is confirmed that the oscillation of both the conductance and the spin polarization is modulated periodically when tuning $U_{g2}$. However, its phase is still unchanged. The oscillation is strong when there are a lot of hole bound states around the Fermi level in gated region 2; otherwise, it is weak. But even in the case of $U_{g2} = 327$ meV, i.e., when the total conductance is small [see Fig. 4(a)], the oscillation of the spin polarization is still significant and can reach a value of about 50%, as shown in Fig. 4(b). This suggests that by tuning $U_{g2}$, one can achieve high spin polarized states with either a high or a low electrical current.

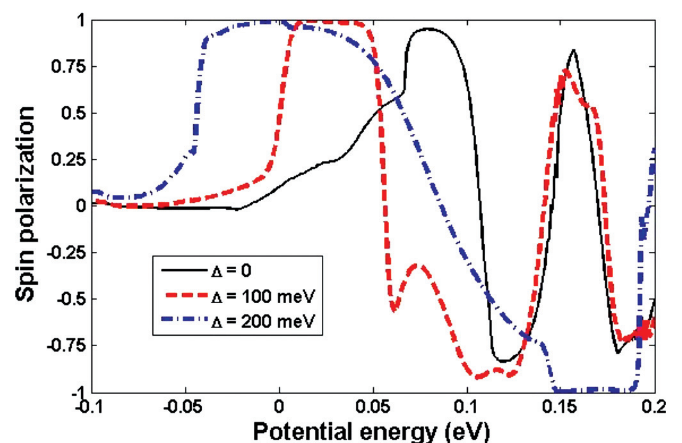


FIG. 3. (Color online) Spin polarization vs the potential energy $U_g$ around the Fermi level for different values of $\Delta$ ($\equiv U_1 - U_2$). The Fermi energy $E_F = 75$ meV, the spin splitting $h = 22.5$ meV, and the gate length $L = 20$ nm.

Author complimentary copy. Redistribution subject to AIP license or copyright, see http://jap.aip.org/jap/copyright.jsp

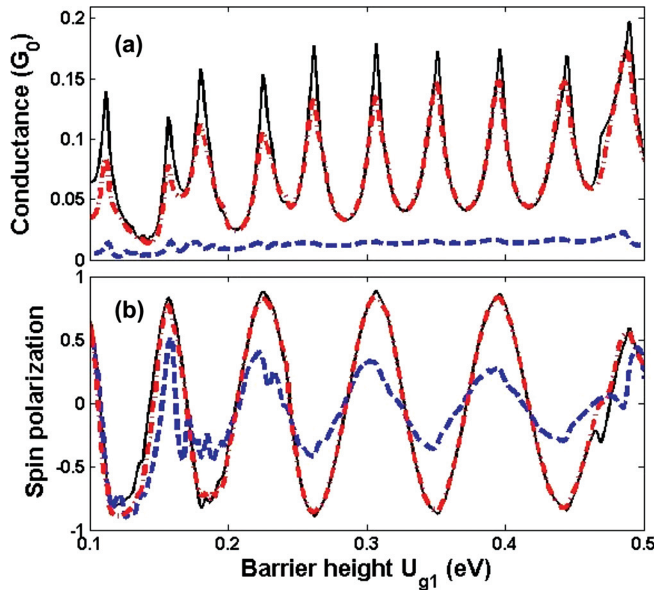


FIG. 4. (Color online) (a) Total conductance and (b) spin polarization vs the barrier height $U_{g1}$ in dual gate structures for different values of $U_{g2}$: 284.5 meV (solid lines), 327 meV (dashed lines), and 370 meV (dotted-dashed lines). The device parameters are $E_F = 75$ meV, $h_1 = 22.5$ meV, $h_2 = 0$, $L_1 = L_2 = 20$ nm, and $d = 50$ nm.

Next, we investigate the spin transport when both gates are ferromagnetic. In this case, the magnetic moment in the first gated region 1 is fixed, while that in the second can be reversed to generate different (parallel or antiparallel) alignment configurations. We therefore can consider the behavior of both the spin polarization of each alignment (for example, parallel) and the TMR as displayed in Fig. 5 for different values of $U_{g2}$. In contrast to the previous cases, Fig. 5(a) shows that when tuning $U_{g2}$, the $P$–$U_{g1}$ curve oscillates between positive and negative values. Though not shown here, the study shows that the similar results are also obtained for the antiparallel alignment; however, the phase difference between two configurations is always $\pi$. Regarding the behavior of TMR, Fig. 5(b) shows that, similar to the spin polarization, the TMR in this structure also has an oscillatory behavior with respect to the barrier height $U_{g1}$, and its amplitude can reach very high values (about 80% to 90% here) in comparison with that in monolayer structures,[37] where the maximum value is only about 10%. However, when tuning $U_{g2}$, both its phase and its amplitude are modulated periodically. The oscillation of the TMR is strongest when the difference between the local densities of states for two spin channels around the Fermi level in gated region 2 is largest, and it is almost fully suppressed when they are equal, as seen in the case of $U_{g2} = 327$ meV in Fig. 5(b).

Another important point, which should be examined, is the possible role of the confined states in the quantum well region (separating the two gate electrodes). Our study shows that, although the confined states exist in the well region [see Fig. 6(a)], the oscillation of the transport quantities (conductance, spin polarization, and TMR) seems to depend weakly on the well's width $d$ in the conduction region ($U_g \gg E_F > 0$); for instance, see the total conductance plotted in Fig. 6(b) as a function of $U_{g1}$. In contrast, the alignment of hole bound states inside the barrier regions plays an important role that determines the pictures of the gate control spin current studied in this work. Similar features in double barrier monolayer graphene structures are discussed in Refs. 37 and 38.

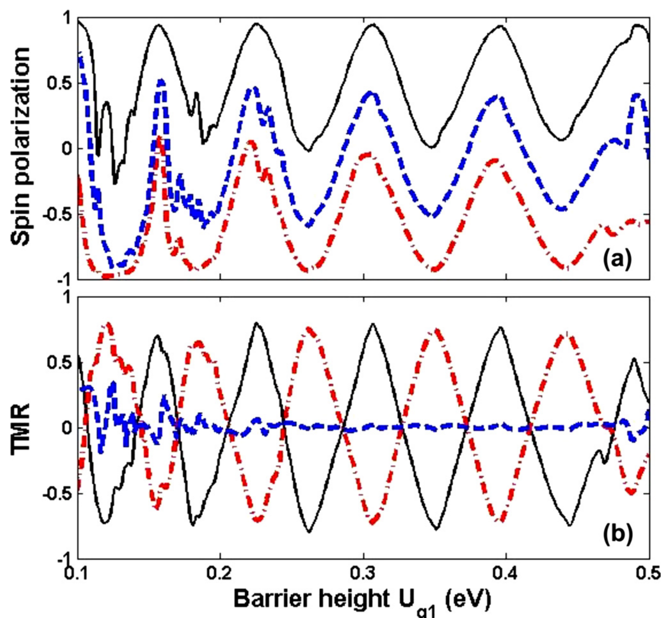


FIG. 5. (Color online) (a) Spin polarization in the case of the parallel alignment and (b) TMR vs the barrier height $U_{g1}$ in dual gate structures for different values of $U_{g2}$: 305.8 meV (solid lines), 327 meV (dashed lines), and 348.5 meV (dotted-dashed lines). The device parameters are $E_F = 75$ meV, $h_1 = h_2 = 22.5$ meV, $L_1 = L_2 = 20$ nm, and $d = 50$ nm.

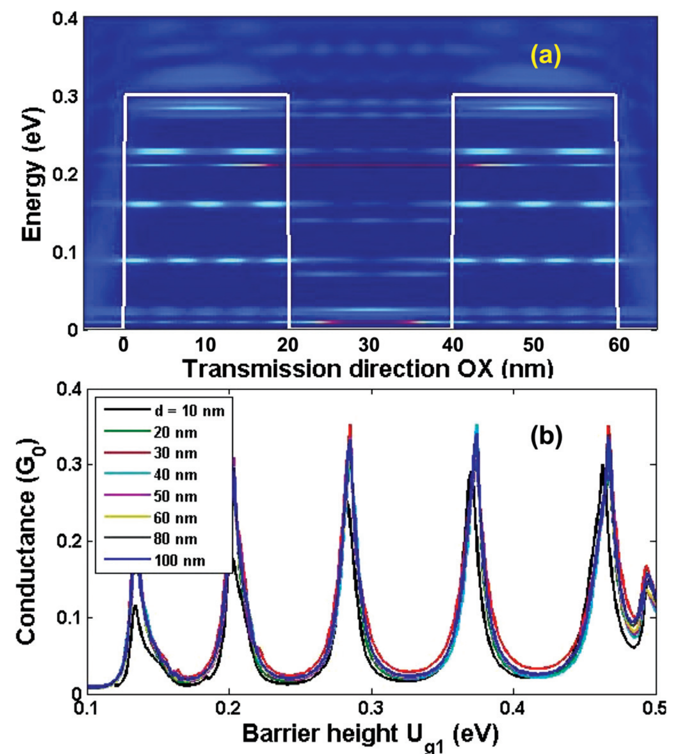


FIG. 6. (Color online) (a) Local density of states plotted for $E_y = 50$ meV clearly showing the picture of charge states in a double barrier structure. (b) Oscillation of total conductance with respect to the barrier height $U_{g1}$ for different well widths. The device parameters are $E_F = 75$ meV, $h_1 = h_2 = 0$, $L_1 = L_2 = 20$ nm, and $U_{g2} = 284.5$ meV.

Author complimentary copy. Redistribution subject to AIP license or copyright, see http://jap.aip.org/jap/copyright.jsp

## IV. CONCLUSION

In conclusion, using the NEGF technique, we have investigated the spin dependent transport in ferromagnetic gate bilayer graphene structures. It is shown that (a) due to the exchange field in the ferromagnetic graphene and to the chiral tunneling through hole bound states in the barrier region, the spin polarization and the TMR have an oscillatory behavior with respect to the barrier height, which can be tuned by the gate voltage; and (b) due to the strong resonant tunneling effects, quantities with very high values in comparison with those in monolayer structures are observed. Some possibilities for controlling the spin current have been discussed, such as the effects of the electric-field-induced energy bandgap and the use of single gate or dual gate structures. We hope that these results will stimulate further developments in graphene-based spintronics.

## ACKNOWLEDGMENTS

The authors would like to thank Van Lien Nguyen for useful discussions. This work was partially supported by the French ANR through the project NANOSIM-GRAPHENE (ANR-09-NANO-016). One of the authors (V.H.N.) acknowledges the Vietnamese NAFOSTED for having supported his work in Hanoi under Project No. 103.02-2010.33.

[1] K. S. Novoselov, A. K. Geim, S. V. Morozov, D. Jiang, Y. Zang, S. V. Dubonos, I. V. Grigorieva, and A. A. Firsov, Science **306**, 666 (2004).
[2] A. Cresti, N. Nemec, B. Biel, G. Niebler, F. Triozon, G. Cuniberti, and S. Roche, Nano Res. **1**, 361 (2008).
[3] A. H. Castro Neto, F. Guinea, N. M. R. Peres, K. S. Novoselov, and A. K. Geim, Rev. Mod. Phys. **81**, 109 (2009).
[4] F. Schwierz, Nat. Nanotechnol. **5**, 487 (2010).
[5] O. V. Yazyev, Rep. Prog. Phys. **73**, 056501 (2010).
[6] P. R. Wallace, Phys. Rev. **71**, 622 (1947).
[7] K. I. Bolotin, K. J. Sikes, Z. Jiang, M. Klima, G. Fudenberg, J. Hone, P. Kim, and H. L. Stormer, Solid State Commun. **146**, 351 (2008).
[8] C. L. Kane and E. J. Mele, Phys. Rev. Lett. **95**, 226801 (2005).
[9] K. S. Novoselov, A. K. Geim, S. V. Morozov, D. Jiang, M. I. Katsnelson, I. V. Grigorieva, S. V. Dubonos, and A. A. Firsov, Nature **438**, 197 (2005).
[10] K. S. Novoselov, E. McCann, S. V. Morozov, V. I. Fal'ko, M. I. Katsnelson, U. Zeitler, D. Jiang, F. Schedin, and A. K. Geim, Nat. Phys. **2**, 177 (2006).
[11] M. I. Katsnelson, K. S. Novoselov, and A. K. Geim, Nat. Phys. **2**, 620 (2006).
[12] N. Tombros, C. Jozsa, M. Popinciuc, H. T. Jonkman, and B. J. van Wees, Nature **448**, 571 (2007).
[13] N. M. R. Peres, F. Guinea, and A. H. Castro Neto, Phys. Rev. B **72**, 174406 (2005).
[14] O. V. Yazyev and L. Helm, Phys. Rev. B **75**, 125408 (2007).
[15] Y.-W. Son, M. L. Cohen, and S. G. Louie, Nature (London) **444**, 347 (2006).
[16] Y. G. Semenov, K. W. Kim, and J. M. Zavada, Appl. Phys. Lett. **91**, 153105 (2007).
[17] H. Haugen, D. Huertas-Hernando, and A. Brataas, Phys. Rev. B **77**, 115406 (2008).
[18] M. Wimmer, I. Adagideli, S. Berber, D. Tomanek, and K. Richter, Phys. Rev. Lett. **100**, 177207 (2008).
[19] W. Y. Kim and K. S. Kim, Nat. Nanotechnol. **3**, 408 (2008).
[20] F. Muñoz-Rojas, J. Fernandez-Rossier, and J. J. Palacios, Phys. Rev. Lett. **102**, 136810 (2009).
[21] T. Yokoyama, Phys. Rev. B **77**, 073413 (2008).
[22] V. Nam Do, V. Hung Nguyen, P. Dollfus, and A. Bournel, J. Appl. Phys. **104**, 063708 (2008).
[23] J. Zou, G. Jin, and Y.-Q. Ma, J. Phys.: Condens. Matter **21**, 126001 (2009).
[24] V. Hung Nguyen, V. Nam Do, A. Bournel, V. Lien Nguyen, and P. Dollfus, J. Appl. Phys. **106**, 053710 (2009).
[25] V. Hung Nguyen, V. Nam Do, A. Bournel, V. Lien Nguyen, and P. Dollfus, J. Phys.: Conf. Ser. **193**, 012100 (2009).
[26] V. Hung Nguyen, A. Bournel, V. Lien Nguyen, and P. Dollfus, Appl. Phys. Lett. **95**, 232115 (2009).
[27] V. Hung Nguyen, A. Bournel, and P. Dollfus, J. Phys.: Condens. Matter **22**, 115304 (2010).
[28] G. Fiori and G. Iannaccone, IEEE Electron Device Lett. **30**, 261 (2009).
[29] F. Xia, D. B. Farmer, Y.-M. Lin, and P. Avouris, Nano Lett. **10**, 715 (2010).
[30] M. P. Lopez Sancho, J. M. Lopez Sancho, and J. Rubio, J. Phys. F: Met. Phys. **14**, 1205 (1984).
[31] S. Roche, Nat. Nanotechnol. **6**, 8 (2011).
[32] In wide graphene sheets, the most remarkable change in the electronic structure induced by the disorder appears at the K-point ($E_F$=0), where it can give rise to localized states [see M. A. H. Vozmediano, M. P. López-Sancho, T. Stauber, and F. Guinea, Phys. Rev. B **72**, 155121 (2005)]. Therefore, we assume that its effects can be negligible when considering the transport at a finite energy ($E_F$=75 meV in this work).
[33] M. R. Masir, P. Vasilopoulos, A. Matulis, and F. M. Peeters, Phys. Rev. B **77**, 235443 (2008); M. R. Masir, P. Vasilopoulos, and F. M. Peeters, Appl. Phys. Lett. **93**, 242103 (2008).
[34] M. R. Masir, P. Vasilopoulos, and F. M. Peeters, Phys. Rev. B **82**, 115417 (2010).
[35] J. B. Oostinga, H. B. Heersche, X. Liu, A. F. Morpurgo, and L. M. K. Vandersypen, Nature Mater. **7**, 151 (2008).
[36] M. Barbier, P. Vasilopoulos, and F. M. Peeters, Phil. Trans. R. Soc. London, Ser. A **368**, 5499 (2010).
[37] V. H. Nguyen, A. Bournel, P. Dollfus, and V. L. Nguyen, J. Phys.: Conf. Ser. **187**, 012037 (2009).
[38] J. M. Pereira, Jr., P. Vasilopoulos, and F. M. Peeters, Appl. Phys. Lett. **90**, 132122 (2007).

**Author complimentary copy. Redistribution subject to AIP license or copyright, see http://jap.aip.org/jap/copyright.jsp**